

Impact of UGT80B1 absence on *Arabidopsis thaliana* growth under salt stress

Manoj Kumar Mishra*, Ajay Kumar, Vivek Srivastava

Faculty of Engineering & Technology, Rama University Kanpur UP

Corresponding Author- Manoj Kumar Mishra,

[Email- manoj.fet@ramauniversity.ac.in](mailto:manoj.fet@ramauniversity.ac.in),

Abstract

Sterol glycosylation, facilitated by sterol UDP-glycosyltransferases (SGTs), plays a crucial role in various biological functions, influencing cellular homeostasis, lipid metabolism, water solubility, molecule stability, and the properties of cell membranes for improved transport system access and stress tolerance. In the model plant *Arabidopsis thaliana* (*A. thaliana*), two sterol β -glucosyltransferase genes within the UGT80 subfamily, UGT80B1 (At1g43620) and UGT80A2 (At3g07020), are responsible for catalyzing the glycosylation of the 3β -hydroxy group of sterols, resulting in the formation of 3β -D-glycosides. Analysis of knockout mutants for both genes, particularly salk-021175 (Atg43620 gene), revealed a moderate impact on growth under normal conditions, with a distinctive transparent seed coat compared to other genotypes. However, under salt stress, this knockout mutant exhibited significant adverse effects on overall plant growth, physiological activities, and enzyme functions compared to other genotypes. The relative expression of *AtSGTs* under salt stress, along with chlorophyll fluorescence analysis, emphasized the crucial role of the Atg43620 gene in both normal plant growth and stress responses. Overall, the findings underscore the importance of sterol glycosylation, particularly mediated by the Atg43620 gene, in shaping plant physiology and enhancing stress tolerance.

Key words Sterol glycosyltransferase, Knockout mutants. Salt stress, Chlorophyll fluorescence, Electrolyte conductivity.

Introduction

Glycosyltransferases (GTs) are pivotal enzymes responsible for the glycosylation of various plant compounds. These enzymes facilitate the transfer of single or multiple activated sugars from nucleotide sugar donors to a diverse range of small molecular acceptors in plants. The most common acceptors are molecules with a 3β -hydroxy group, while UDP-glucose serves as the most prevalent donor (Bouvier-Nave et al., 1984, Mishra et al., 2021). Glycosylation is considered a crucial modification reaction for plant secondary metabolites, contributing significantly to cell homeostasis. This process likely plays a key role in regulating plant growth, development, and defense responses to stress environments (Chaturvedi et al., 2011; Mishra et al., 2022). Research on glycosyltransferases and glycosylation in low-molecular weight plant compounds has primarily focused on *Arabidopsis thaliana* and other plant species. The combination of biochemical and genomic data on plant GTs has enabled the exploration of their biological roles using functional genomics techniques, including gene over-expression and knockout/knockdown strategies.

In the genome of *A. thaliana*, two sterol β -glucosyltransferase genes in the UGT80 subfamily, namely UGT80B1 (At1g43620) and UGT80A2 (At3g07020), catalyze the

glycosylation of the 3 β -hydroxy group of sterols, producing 3 β -D-glycosides. Sterol glycosides (SGs) are crucial membrane components in both prokaryotes and eukaryotes, contributing to membrane fluidity and permeability. A difference in the proportion of glycosylated versus acylated sterols has been observed in different solanaceous species under cold acclimation experiments, suggesting a potential role of SGs in temperature stress adaptation (Palta et al., 1993). Mutation in the UDP-glucose: sterol glucosyltransferase gene (UGT80B1) in *Arabidopsis*, reported by Debolt et al. (2010), resulted in a transparent testa phenotype and suberization defects in seeds. Additionally, gene expression data from microarray experiments indicated a slight up-regulation of At1g43620 (UGT80B1) transcripts in response to cold stress. The mutants presented an opportunity to investigate the expression of At1g43620 and At3g07020 genes under salt stress conditions. Recent functional characterization of *Arabidopsis* sterol glucosyltransferase TTG15/UGT80B1 showed these genes have involvement during freeze and heat stress adaptation plants, which suggests SGTs environmental interactions.

In the present communication, identified *Arabidopsis* mutants with T-DNA inserts in either At1g43620 or At3g07020 gene and determined the effects of the mutations on seed germination, plant growth, development, and gene expression in presence of salt stress. Our findings suggest that the At1g43620 and At3g07020 genes play a crucial role in maintaining normal plant growth and development, and they exhibit a notable influence on the plant's response to salt stress. Differences in the germination percentage and phenotypes of At1g43620 and At3g07020 mutant plants suggested that these proteins of wild-type (WT) have distinct as well as common functions, a conclusion reinforced by gene expression profile analysis. Remarkably, lower germination percentage of Salk-021175 and dramatically altered chlorophyll fluorescence analysis at all concentrations of NaCl, indicating that At1g43620 gene may be involved in modulating the salt tolerance.

Materials and methods

Plant materials

The *Arabidopsis thaliana* lines utilized in this study all belonged to the Columbia background (Col-0). The plants were cultivated in a controlled culture room maintained at 22°C under long day (LD) conditions, consisting of 16 hours of light and 8 hours of darkness, with white light illumination at an intensity of 120 $\mu\text{mol m}^{-2} \text{s}^{-1}$. To ensure uniform conditions, the seeds underwent surface sterilization using a 30% bleach solution and were then stratified for 3 days on 0.15% agar at 4°C. For phenotypic analysis and growth assays, seedlings were exposed to light for 1 hour and subsequently grown either in continuous light or complete darkness at 22°C. The growth medium consisted of plates containing 0.5X Murashige and Skoog's mineral salts (Sigma) and 0.8% agar. The T-DNA insertional sterol glucosyltransferase mutants, namely Salk-021175 (At1g43620) and Salk-109161 (At3g07020), were sourced from a mutant pool available at the Arabidopsis Biological Resource Center (ABRC, Ohio State University, OH). Additionally, the seeds of the p35S:UGT80B1 complementation phenotype of *A. thaliana* were cultivated in our laboratory to ensure consistency in experimental conditions.

Identification of T-DNA Insertions in mutants

The identification of Salk homozygous T-DNA inserted mutant in both At3g07020 (UGT80A2) and At1g43620 (UGT80B1) was carried out by PCR, using previously described method by Mishra et al. (2015). We have used screening primers for At3g07020 resulted in the amplification of 400- and 1000-bp products in mutant and wild-type (WT), respectively, using T-DNA primers LBa1 (5'-TGG TTC ACG TAG TGG GCC ATC G-3'), At3g0702 (Rev) (5'-GGT TCT GGG ATG GGA TCC -3'), and At3g07020 (Fwd) (5'-GGA AGC ACT TCA AAG AAC TAA AC-3'). Screening primers for At1g43620 produced 400- and 1000-bp mutant and WT products, respectively, using T-DNA primers LBa1 (5'-TGG TTC ACG TAG TGG GCC ATC G-3'), At1g43620 (Rev) (5'-TAT AAC TTG TAT GAT GCG CTC TAA G -3'), and At1g43620 (Fwd) (5'-TCA AGG TCG GTG CAC CTG CCT T-3'). The PCR reaction was performed at a 55°C annealing temperature.

Histochemical Analysis

For histochemical analysis, the ability of seeds to uptake salt was assessed by placing them in a 1% tetrazolium red solution at 30°C for 4 to 24 hours, followed by imaging under light microscopy. Additionally, seeds were stained with DMACA reagent (2% DMACA in 3 M HCl/50% methanol) for a week, washed, and examined using light microscopy.

Transcript level analysis

To assess the modulation of AtSGT transcript levels, real-time quantitative PCR (qRT-PCR) was employed. Total RNA samples were extracted from the relevant plant materials using the RNeasy Plant Total RNA Isolation Kit from Qiagen, USA. Prior to qRT-PCR, extensive pre-treatment of total RNA samples was conducted with RNase-free DNase I to eliminate any potential genomic DNA contamination. Subsequently, first-strand cDNA was synthesized from 2 µg of total RNA in a 20 µl reaction volume using Superscript II reverse transcriptase from Invitrogen. For normalization purposes, the AtSGT gene expression levels were normalized to Actin (At3g18780), serving as an internal housekeeping gene control. Additionally, -RT (no reverse transcription) and non-template controls were included in the analysis. All qRT-PCR runs were replicated at least three times, and a representative result was presented for each individual assay. This rigorous approach ensured the reliability and consistency of the gene expression data obtained from the qRT-PCR experiments.

Salt stress treatment

Seeds from wild-type (WT) Arabidopsis plants, knockout mutants, and p35S:UGT80B1 complemented lines of *A. thaliana* were germinated on ½ MS media containing 2% sucrose and 0.85% agar. The germination took place in a controlled culture room set at 22°C under long-day (LD) conditions, with 16 hours of light and 8 hours of darkness, provided by fluorescent tubes at an intensity of 120 µmol m⁻² s⁻¹. To induce salt stress, NaCl was added to the growth medium at concentrations of 50, 100, 150, and 200 mM, while water (0 mM NaCl) was used as the control. The parameters observed included: 1) germination percentage, 2) root length, 3) fresh weight, 4) dry weight, and 5) chlorophyll content. Transcript levels of

both the At1g43620 and At3g07020 genes were assessed by real-time PCR under normal conditions in 14-day-old WT plants grown on ½ MS media with 0 (water), 50, and 100 mM NaCl for 24 hours. This experimental setup allowed for the comprehensive evaluation of the impact of salt stress on various growth and physiological parameters, as well as the gene expression profiles in the different Arabidopsis lines.

Relative electrolytic conductivity

After salt stress the relative electrolyte conductivity (REC) was measured for all phenotypes to assess stress adaptation (Mishra et al. 2013). REC was measured for each sample with a conductivity meter before and after autoclaving (121°C for 20 min). Fully developed leaves of salt treated or non-treated plants were excised from the base of the petiole and placed in 13x100 mm glass tubes containing 100 µl of deionized water. The tube containing the solution was shaken and left overnight at 24°C. The conductivity of the solution was measured in each tube and the tubes were capped (to minimize evaporation), autoclaved and cooled. After autoclaving, the conductivity of the solution was again measured in each tube. The percentage of electrolyte leakage was calculated as the ratio of the conductivity before autoclaving to that after autoclaving. It is assumed that the conductivity after autoclaving represents complete (100%) electrolyte leakage.

Measurements of oxidative stress, SOD enzyme activity, and relative electrolytic conductivity

Total amount of SOD enzyme was estimated as a function of NBT reduction using spectrophotometer. Leaf samples (250 mg) from the seedlings were homogenized in a precooled mortar in homogenizing buffer containing 0.1 mM EDTA, 0.5% (v/v) Triton-X 100 and 1% (w/v) PVP in 100 mM phosphate buffer (pH 7.8). The homogenate was transferred to 1.5 ml Eppendorf tubes and centrifuged at 13,000 rpm for 20 min at 4°C. The supernatant was collected and total SOD levels were estimated according to Beyer and Fridovich (1987). Protein content was estimated according to the dye binding method of Bradford (1976). The total SOD activity was measured by adding 20 µl supernatant to a reaction mixture containing 4.4% (w/v) Riboflavin, 57 µM NBT, 10 mM L-Methionine and 0.025% (v/v) Triton-X 100 in 100 mM phosphate buffer. One unit of enzyme activity was defined as the amount of enzyme required for 50% inhibition of NBT reduction in 2 min at 25°C.

Chlorophyll estimation of all phenotypes

Estimation of chlorophyll in all normal grown plants and treated plants was done by Ritchie (2008) protocol. In the present study, 80% acetone was used for determination of chlorophyll and absorption was recorded at 645 and 663 Å.

Chlorophyll fluorescence measurements for finding the effect of transgene

An Imaging-PAM, M-Series Chlorophyll Fluorometer (Walz, Effeltrich, Germany), was used to study the chlorophyll fluorescence parameters (Ehlert and Hinch, 2008). Calculations of various chlorophyll fluorescence parameters were done according to Maxwell and Johnson

(2000). The maximum photochemical efficiency of photosystem II (PSII), (F_v/F_m : where F_m is maximum fluorescence of the dark-adapted leaf under a light saturating flash and F_v is maximum variable fluorescence, $F_m - F_0$) was measured on leaves after 20 min of dark adaptation. The effective quantum yield of PSII (Y) was calculated as $(F_m - F_s)/F_m$. NPQ is a non-photochemical quenching measurement that indicates a change in efficiency of excess excitation energy dissipation by heat. NPQ collectively indicates heat dissipation triggered by low thylakoid lumen pH, state transitions of PSII centers, and photo inhibition. $Y(NPQ)$ is a measure of the fraction of photons absorbed by PSII antennae. Increased NPQY is an indication of protective strategies at PSII. $Y(NO)$ is the fraction of photons dissipated by dissociation of light-harvesting complex II and indicates irreversible PSII damage.

Results

T-DNA insertion lines for this study was taken from previously studied mutant *Arabidopsis* lines. Salk-021175, contained T-DNA insertion at the fifth exon, downstream of the translational initiation codon, while, Salk-109161, contained a T-DNA insertion in the intron, 702 bp downstream of 5' UTR region (Fig.1a-b). Homozygous lines carrying T-DNA mutations in Salk-109161 and Salk-021175 were isolated by PCR analysis with kanamycin selection (Fig.1c). Reverse transcriptase (RT)-PCR analysis using primers that span the T-DNA insertion confirmed the absence of full-length mRNA (Fig.1e-d). Homozygous Salk-021175 mutant plants showed the effects of absence of this gene at several stages of plant development. The Salk-021175 phenotype was characterized by normal height, light green color and twisted (curled) leaves as compared to WT (Fig. 2b). Also, inflorescence stems of this mutant were smaller than those of WT plants (Fig. 2b). The root systems in Salk-021175 plants were shorter than that in WT plants, with an ectopic root hair (Fig. 2n and 3b). The floral organs, particularly petals and stamens, were also affected in Salk-021175 plants. The flowers opened maturely, with small petals that curled outward and stamens were shorter than the carpels in both the knockout mutants as compared to WT as well as *35S:UGT80B1* (Fig. 2e-h). The leaves of the rosette of homozygous mutant plants were smaller than WT leaves (Fig. 2b and c). Thus, the fertilization of homozygous mutant plants resulted in small siliques having less number of seeds (Fig. 2j). The most notable phenotypic feature was, Salk-021175 displayed a transparent testa phenotype and a reduction in seed size (Fig. 3f). Homozygous Salk-109161 plants were also identified and confirmed by PCR. The phenotypes of Salk-109161 homozygotes did not resemble the Salk-021175. Some phenotype resembled, in root growth (Fig. 2o), the size of rosette and the adult plant (Fig. 2c), and the tissue-specific deformities in flowers (Fig. 2g). A phenotypic feature of rescued *p35S::UGT80B1* line was almost similar to WT but growth of plants was retarded as compared to WT (Figs. 2d, h, I and p; Fig. 3d, h and i).

Histochemical and microscopic analysis of seeds

A visual inspection showed that seeds of Salk-021175 mutant were reduced in size and seed coat was light in color as compared to WT. On the contrary, in Salk-109161 mutant, although seed size was relatively smaller as compared to WT but seed coat was dark brown similar to WT. To know the possible reason for increased permeability of Salk-021175 (*Atlg43620*)

seeds, we have done a series of histochemical and microscopic analysis of seeds similar to Debolt et al. (2010). When seeds were treated in a solution of tetrazolium salt, Salk-021175 seeds were observed to be highly sensitive to salt uptake but unable to limit uptake and entire seeds became stained with dark red color (Fig. 3f), whereas WT and Salk-109161 seeds absorbed small amount of salt (Fig. 3e, g). Phenotype of *p35S:UGT80B1* seeds behaved like WT means absorbed small amount of salt (Fig. 3h). Pigmentation of the seed coat was determined by the deposition of flavanoids using 4-dimethylamino cinnamaldehyde (DMACA) reagent. Consistent with the transparent testa phenotype, the most drastic reduction in DMACA staining was in Salk-021175 mutant (Fig. 3j), while the seeds of Salk-109161 mutant showed contrasting results (Fig. 3k). The DMACA staining phenotype of *p35S::UGT80B1* seeds were also rescued (Fig. 3i).

Expression analysis of *At1g43620* and *At3g07020* transcripts under salt stress

In silico data suggested that *At1g43620* and *At3g07020* were expressed under salt treatments and cold stress conditions. To assess whether *At1g43620* and *At3g07020* were actually expressed under salt stress, qRT-PCR analysis was performed by using *At1g43620* and *At3g07020* specific primers after salt treatments on 14-days-old seedlings. As shown in Fig. 4, *At1g43620* was expressed relatively more 3.5 fold at 50 mM NaCl (for 24 h). When the salt concentration increased upto 100 mM NaCl transcripts gradually decreased in 24 h. In contrast, *At3g07020* transcript level has not shown the impressive expression at both the salt concentrations. These results indicated that *At1g43620* gene was induced by little amount of salt stress conditions, whereas, *At3g07020* gene did not respond to salt stress conditions.

Effect of salt stress on mutant Salk-021175, Salk-109161 and *p35S:UGT80B1* plants

We evaluated the phenotypic and physiological changes that occurred in mutants and complemented plants of *A. thaliana* under salt stress. Both mutant lines and *p35S:UGT80B1* complemented lines germinated well at 50 and 100 mM NaCl (Fig. 5a). At higher concentration of NaCl (150 mM and 200 mM), there was no germination of mutant Salk-021175 but Salk-109161 showed poor germination, in contrast to WT seeds and *p35S:UGT80B1* complemented lines which showed remarkably high germination (Fig. 5a). Germination percentage was calculated as number of seeds germinated per sixty seeds. Also, at 100 mM of NaCl, the germination of both the mutants was delayed. The cotyledons of Salk-109161 seedlings were smaller, yellowish green and epinastic, whereas Salk-021175 seedlings were although smaller but yellow in color (Fig. 6). The hypocotyls of the mutant seedlings were shorter than the WT hypocotyls (Fig. 6). Root length of Salk-021175 knockout mutant plants was significantly less as compared to WT plants (Fig. 5b). Root length of Salk-109161 knockout mutant plants was not significantly less as compared to WT plants upto 100 mM NaCl but at higher concentrations (150 mM and 200 mM) root length significantly decreased (Fig. 5b). Root length of *p35S:UGT80B1* complemented lines was significantly more than Salk-021175 mutant and almost similar like WT (Fig. 5b). Fresh weight/dry weight (both fresh weight and dry weight were measured to ascertain the biomass) and number of true leaves were more in *p35S:UGT80B1* complemented lines - than both of the knockout mutants (Fig. 5c-d). These results suggested that Salk-021175 mutants'

germination, root growth, fresh weight, dry weight and total chlorophyll were more affected under salt stress conditions as compared to normal medium, its complemented phenotype rescued similar phenotypic pattern like WT.

Differential effects of salt treatments on chlorophyll and fluorescence response (Fv/Fm)

Chlorophyll measurement showed more dramatic chlorophyll loss in the mutant leaf disks than the WT and *p35S:UGT80B1* complemented lines under salt stress. There was no significant difference in chlorophyll contents between knockout mutant, and *p35S:UGT80B1* complemented lines without treatment while chlorophyll content was slightly more in WT. However, in the presence of 100 mM NaCl, there was 95% chlorophyll loss in Salk-021175 and 94% chlorophyll loss in Salk-109161 mutant leaf disks, but only 46% in complemented phenotypes – the discrepancy was greater with increased NaCl concentrations (Fig. 7a). Additionally, further chlorophyll fluorescence imaging has been shown under the selected fluorescence parameters. Variability of the fluorescence response (Fv/Fm) has been shown under salt stress. Under normal conditions, all the phenotypes showed approximately similar fluorescence response while under salt stress, fluorescence response gradually decreased in knockout mutant as compared to WT and *p35S:UGT80B1* complemented lines (Fig.7b). These results suggested that expression of *p35S:UGT80B1* in *Arabidopsis* greatly enhanced its photosynthetic abilities and fluorescence response under salt stress.

Measurement of oxidative stress

The *p35S:UGT80B1* complemented lines expressing the *At1g43620* protein remained green but both knockout mutants were wilted when exposed to higher NaCl in comparison to WT plants. The visual observations were confirmed by measuring SOD activity under normal conditions and after three weeks of growth on 100 mM NaCl. Under normal conditions, the level of SOD was almost similar in all the phenotypes as compared to WT plants. Under salt stress, the level of SOD increased in all the phenotypes but in Salk-021175 mutant, SOD activities were not increased remarkably (Fig. 7c). The percentage SOD activity was less in Salk-021175 knockout as compared to WT. It was 12% and 56.94% under 50 mM and 100 mM NaCl, respectively, but in case of *p35S:UGT80B1*, SOD activity increased upto 24% more than in WT, whereas, it was less in 100 mM NaCl upto 20% as compared to WT. SOD activities in Salk-109161 mutant increased under both the salt concentrations but it was comparatively more than Salk-021175 mutant. The results showed that under salt stress, the SOD activity of Salk-021175 was slightly increased in comparison to normal conditions. Whereas, in *p35S:UGT80B1* lines and Salk-109161 mutants, the increase was more in SOD activity under salt stress as compared to normal conditions. Additionally, comparison of REC between knockout mutant, complemented lines and WT plants showed that at 100 mM NaCl, Salk-021175 plants had a higher REC (101%) than the other phenotypes while Salk-109161 had (67%) REC. (Fig. 7d). Complementated *p35S:UGT80B1* lines and WT plants showed significantly lower REC as compared to knockout mutants after salt stress. Higher SOD activity and lower relative electrolytic conductivity (REC) reflected that *p35S:UGT80B1* lines were adapted to salt stress.

Discussion

T-DNA knockout mutations in Salk-021175 (At1g43620 gene) and Salk-109161 (At3g07020 gene) were subjected to phenotypic characterization under both normal and salt stress conditions. Morphological and phenotypic observations revealed that the overall growth, root patterning, flower size, and silique development were slightly affected in both mutant lines due to the absence of the *sgt* gene (Mishra et al. 2015). This observation confirms the significant role of the *sgt* gene in plant growth and silique formation. The occurrence of a transparent testa in Salk-021175 further supported this confirmation. However, At3g07020 did not exhibit any notable phenotype. Specifically, the presence of ectopic root hairs in Salk-021175 strongly indicated the inhibition of *sgt* gene expression, aligning with findings from a previous study (Galway et al. 1994). Glycosylation, catalyzed by a superfamily of glycosyltransferases (GTs), plays a crucial role in modulating the solubility, stability, bioavailability, and bioactivity of various small molecules (Mishra et al. 2013, Mishra et al. 2021, Mishra et al. 2022). This plasticity is integral to the integration of growth, development, and metabolism, contributing to diverse mechanisms that regulate cellular homeostasis (Bowles et al. 2006).

Our study demonstrated that the expression of *Arabidopsis* GT protein enhanced the adaptation of transgenic *p35S:UGT80B1* complemented lines to environmental stress, as the expression of At1g43620 is salt-inducible. This indicates that the At1g43620 gene may be involved in the modulation of sterol glycosides and acyl sterol glycosides in response to environmental stress in *Arabidopsis* (Grill et al. 2010, Mishra et al. 2021). Further investigation into the germination of different phenotypes under various salt stress conditions revealed that Salk-021175 exhibited poor germination compared to other phenotypes. At 200 mM NaCl, Salk-021175 showed no germination, while the complemented line of this mutant, *p35S:UGT80B1*, germinated well across different concentrations of NaCl compared to WT. The germination percentage of Salk-021175 was consistently lower at all NaCl concentrations, indicating the involvement of the At1g43620 gene in seed germination modulation. Other phenotypic characteristics such as root length, fresh weight, dry weight, and chlorophyll content were lower in Salk-021175 mutant compared to other phenotypes, while *p35S:UGT80B1* lines exhibited a better response than WT and Salk-109161. Chlorophyll, crucial for photosynthesis, showed impairment in both light and dark reactions in knockout mutants under stress conditions, as evidenced by lower performance indices of photochemical Y (NPQ) reactions compared to *p35S:UGT80B1* complemented lines and WT *Arabidopsis*. Chlorophyll fluorescence imaging provided spatial information about salt stress damage under salt stress, Salk-021175 plants displayed a lower Fv/Fm ratio compared to other phenotypes. This reduction in the Fv/Fm ratio and Y (II) under salt stress indicated structural and functional disorders in the photosynthetic apparatus, suggesting damage to PSII, consistent with findings in other studies (Lu et al. 2002, Kalaji et al. 2011). In conclusion, our results highlight the enhanced expression of the At1g43620 gene during salt stress, while the At3g07020 gene showed no significant induction under salt stress conditions. However, further research is needed to understand the structural modifications of these genes under different abiotic stress conditions.

Acknowledgements

The Director, Council of Scientific and Industrial Research-National Botanical Research Institute, is gratefully acknowledged by authors for providing the facilities.

Conflict of Interest- Authors has no conflict of interest

Author contribution - MKM designed and conceived the research work and also write the manuscript.

References

1. Beyer WF, Fridovich I (1987) Assaying for superoxide dismutase activity: some large consequences of minor changes in conditions. *Anal Biochem* 161:559-566
2. Bouvier-Nave P, Ullmann P, Rimmel D, Benveniste P (1984) Phospholipid dependence of plant UDP-glucose sterol β -D-glucosyl transferase I. Detergent mediated delipidation by selective solubilization. *Plant Sci Lett* 36:19-27
3. Bowles D, Lim EK, Poppenberger B, Vaistij FE (2006) Glycosyltransferases of lipophilic small molecules. *Annu Rev Plant Biol* 57:567-597
4. Bradford MM (1976) A rapid and sensitive method for the quantitation of microgram quantities of protein utilizing the principle of protein-dye binding. *Anal Biochem* 72:248-254
5. Chaturvedi P, Misra P, Tuli R (2011) Sterol glycosyltransferases--the enzymes that modify sterols. *Appl Biochem Biotechnol* 165:47-68
6. DeBolt S, Scheible WR, Schrick K, Auer M, Beisson F, et al. (2009) Mutations in UDP-Glucose:sterol glucosyltransferase in *Arabidopsis* cause transparent testa phenotype and suberization defect in seeds. *Plant Physiol* 151:78-87
7. Ehlert B, Hinch (2008) Chlorophyll fluorescence imaging accurately quantifies freezing damage and cold acclimation responses in *Arabidopsis* leaves. *BMC Plant method* 4:12
8. Galway ME, Masucci JD, Lloyd AM, Walbot V, Davis RW, Schiefelbein JW (1994) The TTG gene is required to specify epidermal cell fate and cell patterning in the *Arabidopsis* root. *Dev. Biol.* 166:740-754.
9. Grille S, Zaslowski A, Thiele S, Plat J, Warnecke D (2010) The functions of sterol glycosides come to those who wait: Recent advances in plants, fungi, bacteria and animals. *Prog Lipid Res* 49:262-28
10. Kalaji HM, Govindjee, Bosa K, Koscielniak J, Zuk-Golaszewska K (2011) Effects of salt stress on photosystem II efficiency and CO₂ assimilation of two Syrian barley landraces. *Environmental and Experimental Botany* 73:64-72
11. Lu CM, Qiu NM, Lu QT, Wang BS, Kuang TY, et al. (2002) Does salt stress lead to increased susceptibility of photosystem II to photoinhibition and changes in photosynthetic pigment composition in halophyte *Suaeda salsa* grown outdoors? *Plant Sci* 163:1063-1068
12. Maxwell K, Johnson G (2000) chlorophyll fluorescence - A practical guide. *J Exp Bot* 51:659-668

13. Murashige T, Skoog F (1962) A revised medium for rapid growth and bioassays with tobacco tissue cultures. *Physiol Plant* 15:473–479
14. Mishra MK, Chaturvedi P, Singh R, Singh G, Sharma L K, Pandey V, Kumari N, Misra P (2013) Overexpression of *WsSGTL1* gene of *Withania somnifera* enhances salt tolerance, heat tolerance and cold acclimation ability in transgenic *Arabidopsis* Plants. *PLoS ONE* 8(4):e63064
15. Mishra MK, Tiwari S, Misra, P., 2021. Overexpression of *WssgtL3. 1* gene from *Withania somnifera* confers salt stress tolerance in *Arabidopsis*. *Plant Cell Reports*, pp.1-14.
16. Mishra MK, Singh G, Tiwari S, Singh R, Kumari N, Misra P. Characterization of *Arabidopsis* sterol glycosyltransferase *TTG15/UGT80B1* role during freeze and heat stress. *Plant signaling & behavior*. 2015 Dec 2;10(12):e1075682.
17. Mishra MK, Tiwari S, Srivastava M, Awasthi A, Misra P. Ectopic Expression of *WsSGTL3. 1* Gene in *Arabidopsis thaliana* Confers Enhanced Resistance to *Pseudomonas syringae*. *Journal of Plant Growth Regulation*. 2022 Jun;41(4):1871-86.
18. Palta JP, Whitaker BD, Weiss LS (1993) Plasma membrane lipids associated with genetic variability in freezing tolerance and cold acclimation of *Solanum* species. *Plant Physiol* 103:793-803
19. Ritchie RJ (2008) Universal chlorophyll equations for estimating chlorophylls a, b, c, and d and total chlorophylls in natural assemblages of photosynthetic organisms using acetone, methanol, or ethanol solvents. *Photosynthetica* 46 (1):115-126

Figures

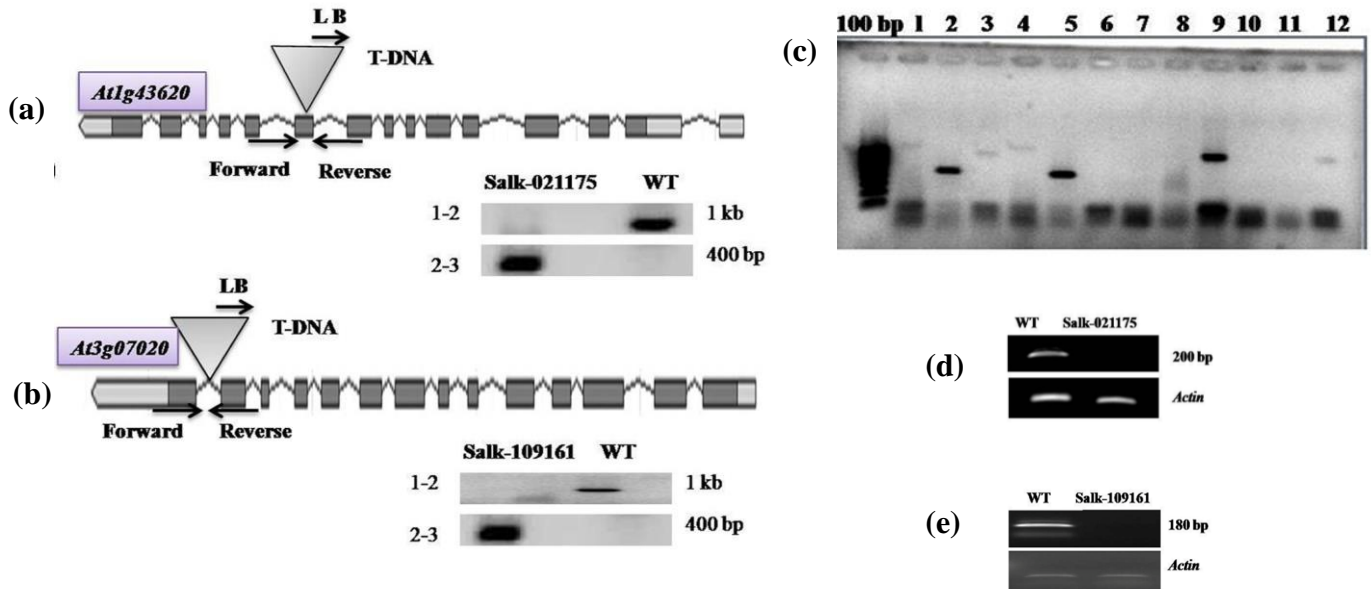


Fig. 1 Molecular characterization of Salk-021175 and Salk-109161 mutants. (a) Scheme of the T-DNA insertion in salk-021175 mutant, indicating the relative positions of exons (gray boxes) and introns (gaps). T-DNA insertion at fifth exon. (b) Scheme of the T-DNA insertion in salk -109161 gene, indicating the relative positions of exons (gray boxes) and introns (gaps). T-DNA insertion at intron. (c) PCR analysis for screening of homozygous line. Lane 2 and 5 represents homozygous line carrying T-DNA insertion in both alleles, while Lane 9 represents WT. (d) RT-PCR analysis, of Salk-021175 mutant (e) RT-PCR analysis, of Salk-109161 mutant primers that flank the T-DNA insertion sites.

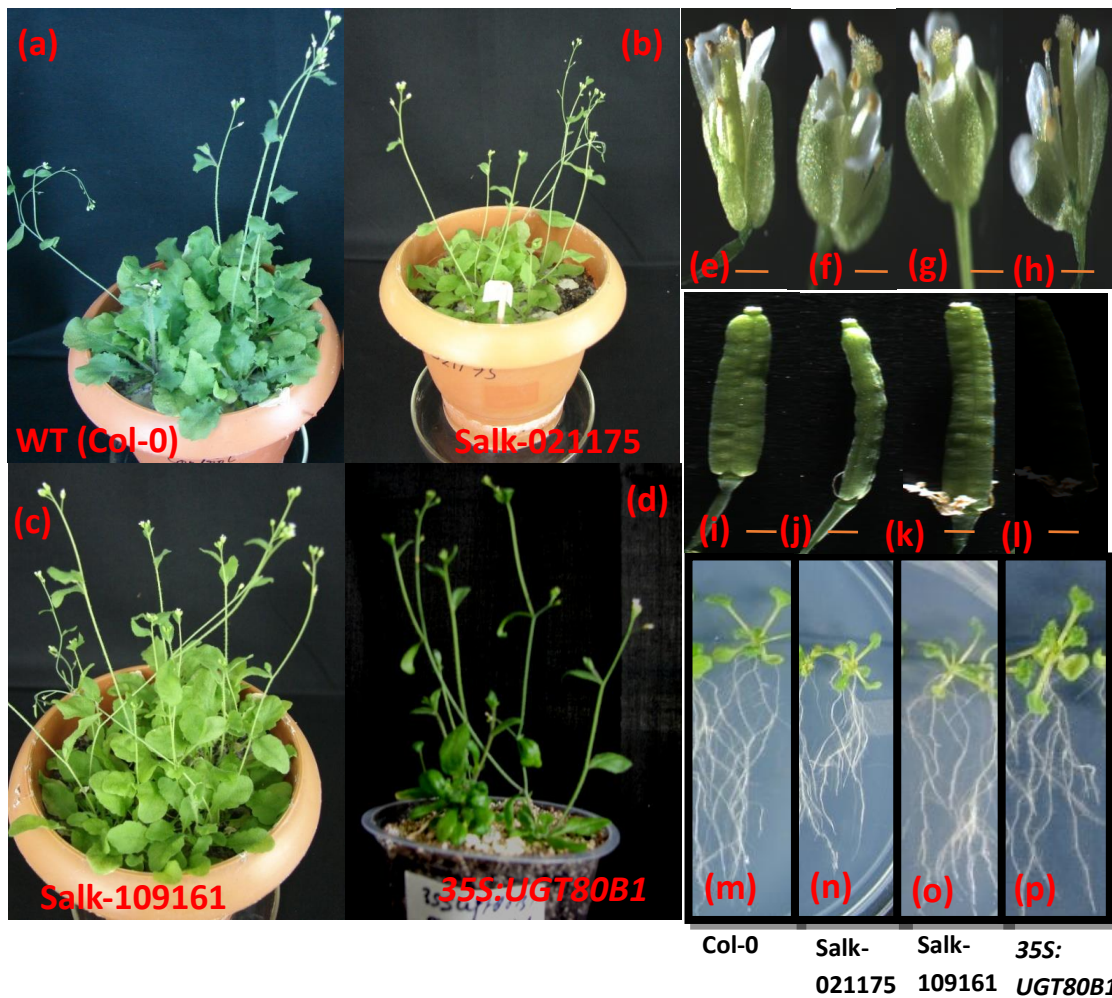


Fig. 2. Phenotypic difference in WT (Col-0), homozygous mutants (Salk-021175, Salk-109161) and complementation line of *A. thaliana* (35S:UGT80B1). (a-d) Five-weeks-old potted plants. (e-h) Flowers showing petals and shorter stamens than the carpels (i-l) Siliques, smaller size in mutants with lesser number of seeds. (m-p) Seedlings at 14-days of growth on agar plates.

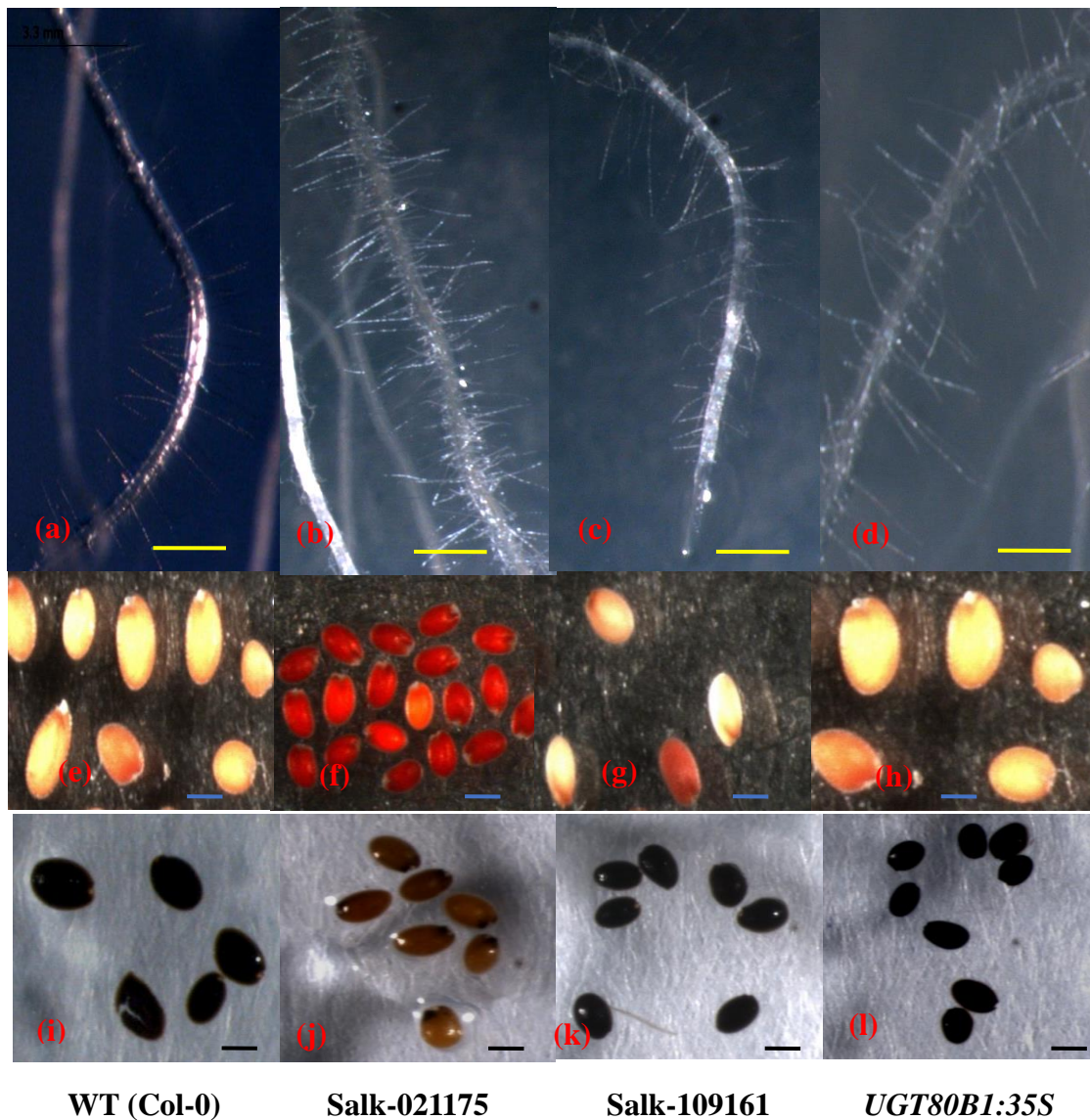


Fig. 3 Phenotypic difference in root and leaf and histochemical analysis of seeds in WT, homozygous mutants and complementation line of *A. thaliana* (a-d) Seedlings roots showing ectopic root hair in Salk-021175 mutant (e-h) Staining by tetrazolium salt. Salk-021175 (f) was displayed with a transparent testa phenotype. (i-l) DMACA staining showing altered deposition of flavonoid on seed coat. Light colour in Salk- 021175.

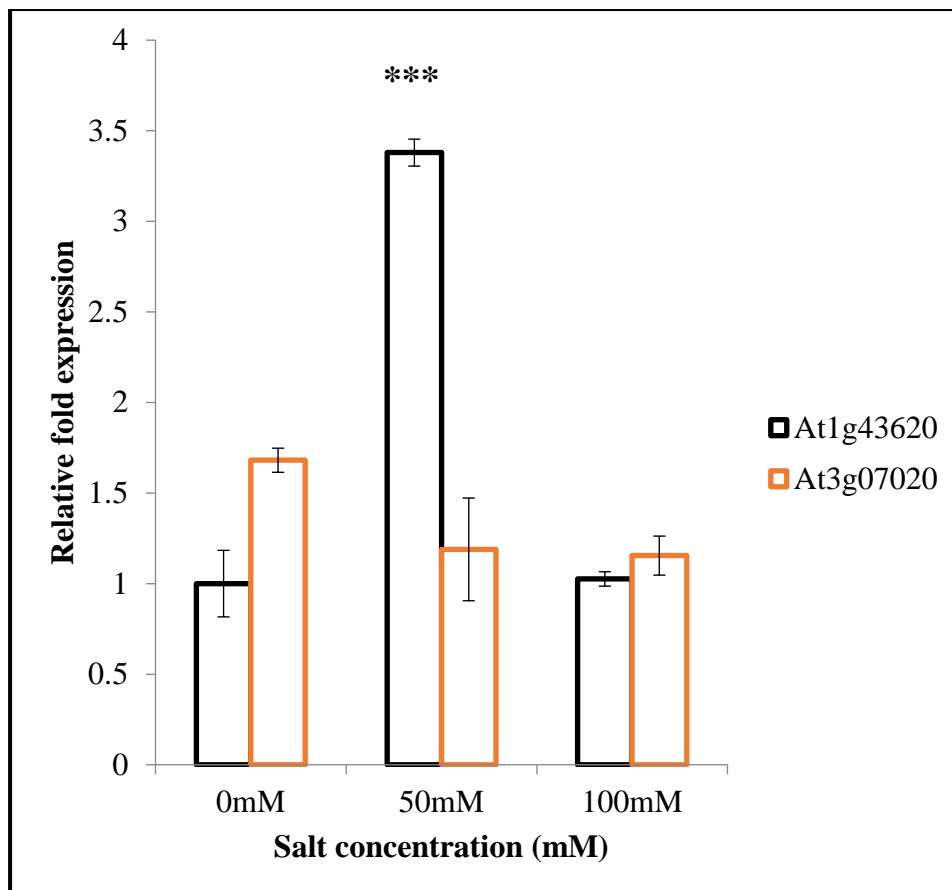


Fig. 4. Real Time PCR analysis- Relative expression of *At1g43620* and *At3g07020* gene under 50 mM and 100 mM salt stress, 0 mM NaCl or water acted as control.

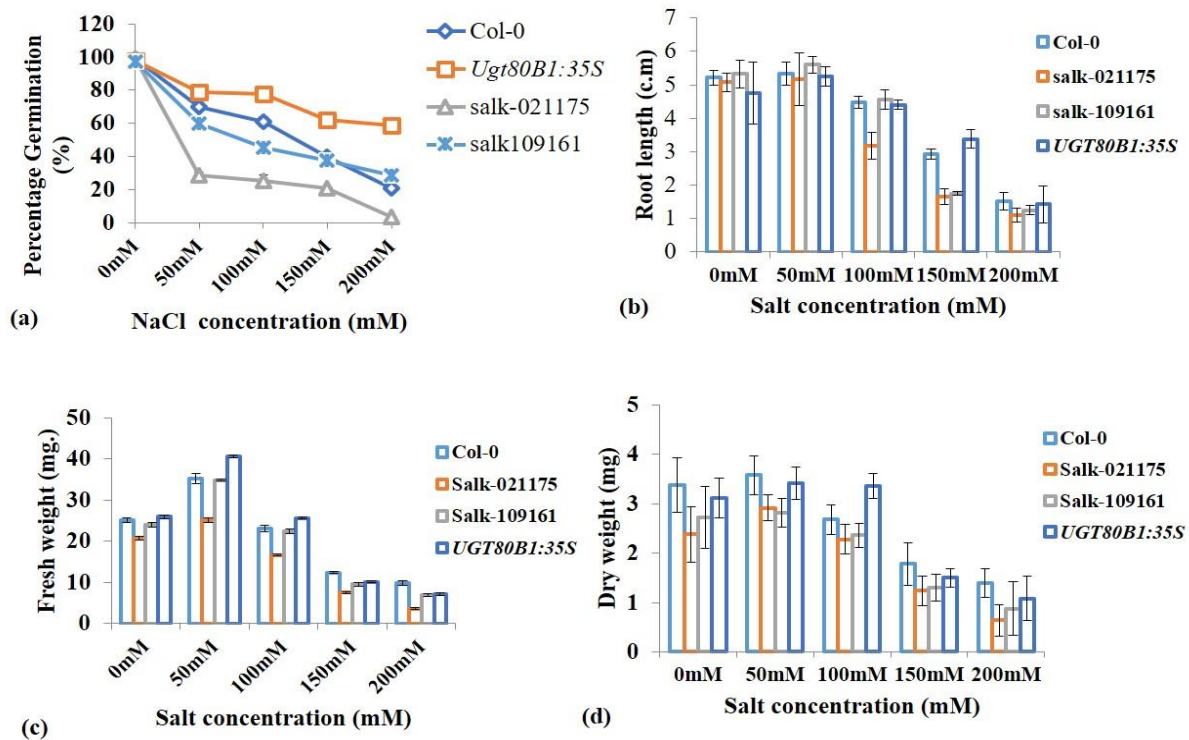


Fig. 5. Effect of salt stress on WT, Salk-021175, Salk-109161 mutants and p35S:UGT80B1 plants. (a) Germination percentage of seeds up to 7 days in 0, 50, 100, 150 and 200 mM salt concentrations, 0 mM represent $\frac{1}{2}$ Ms without NaCl. **(b)** Root length of 14-day-old seedlings in different salt concentrations. **(c)** Fresh weight of whole plants measured after 14-days of salt stress. Values are mean \pm SE, n= 0. **(d)** Dry weight of whole plants measured after 14-days of salt stress. Values are mean \pm SE, n=10.

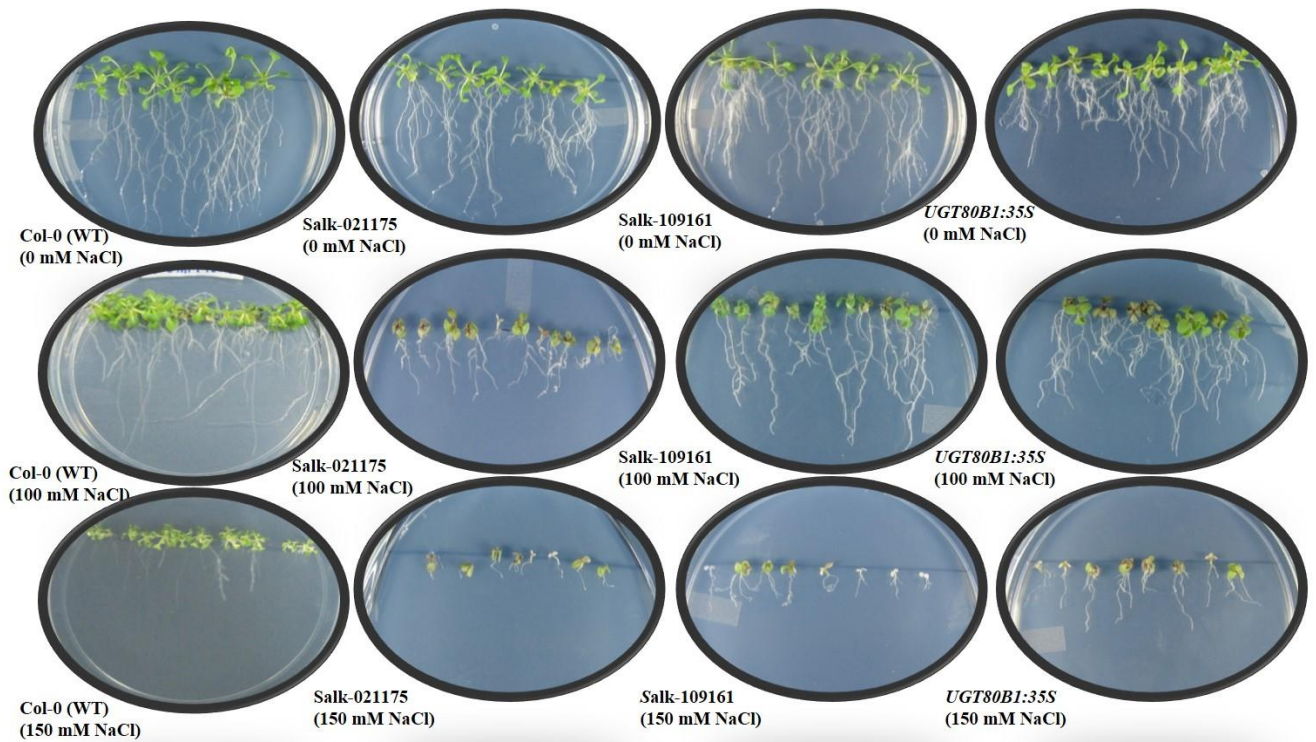


Fig. 6. Phenotypic difference in WT, homozygous mutants and complementation line of *A. thaliana* (From L to R) WT (Col-0), Salk-021175, Salk-109161 and 35S:UGT80B1 under salt stress. (a) Comparison of shoot length, root growth and leaf growth on MS medium. (b) With 100 mM NaCl. (c) With 150 mM NaCl. Photographs were taken after 14 days of germination.

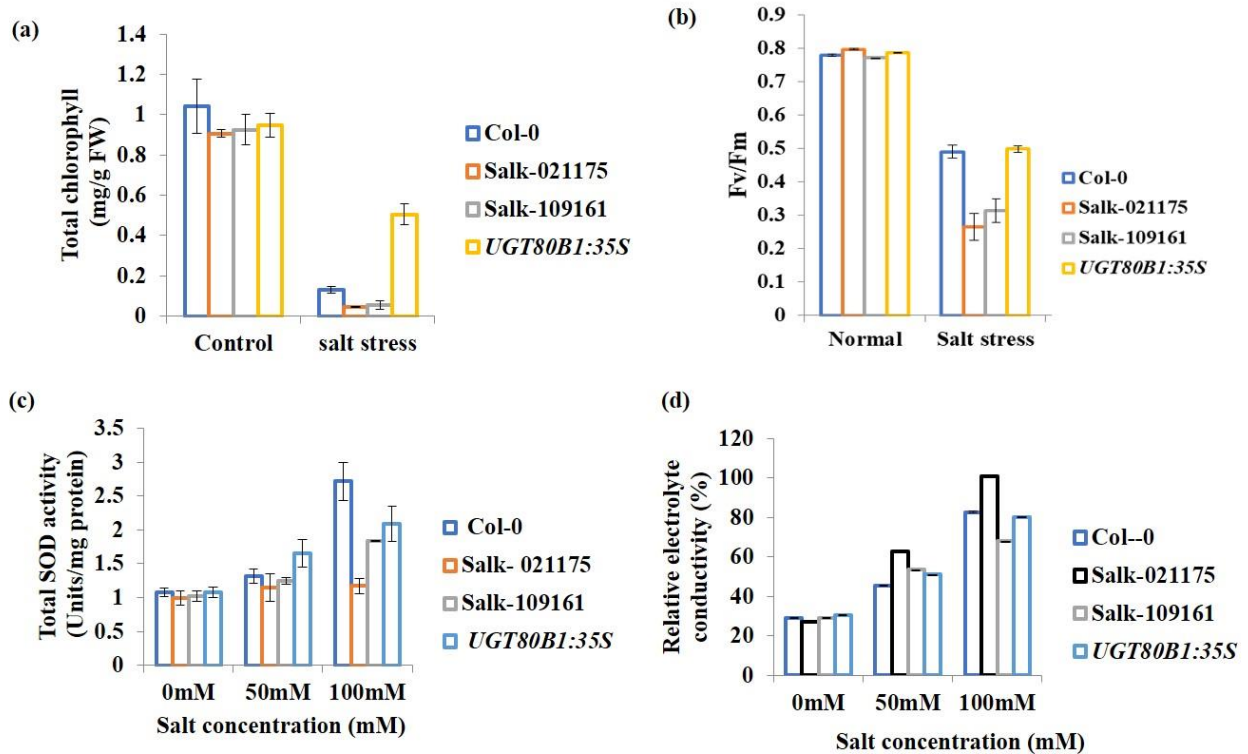


Fig. 7. Chlorophyll contents, Fv/Fm measurements, SOD activity and relative electrolyte conductivity. (a) Total chlorophyll, estimated from equal amount of leaf samples (triplicate in each sample), with and without salt treatment (100 mM NaCl) were represented as mg g⁻¹ FW. Values are the mean \pm SE for three observations. (b) SOD activity analysis in WT (Col-0), Salk-021175, Salk-109161 and 35S:UGT80B1 under 0, 50 and 100 mM salt stress. Values are expressed as mean (n = 3); errors bars show the SD for each experiment. (c) REC analysis under 0, 50 and 100 mM salt stress. Values are expressed as mean (n=3); error bars show SD. (d) Fv/Fm values in WT (Col-0), Salk-021175, Salk-109161 and 35S:UGT80B1 under normal growth condition, salt stress (100 mM) and cold treatment (4°C). Values are expressed as mean (n = 3); error bars show SD for each experiment.